33rd Annual International Conference of the IEEE EMBS
Boston, Massachusetts USA, August 30 - September 3, 2011

EEG Spectro-Temporal Modulation Energy: a New Feature for Automated Diagnosis of Alzheimer's Disease

Lucas R. Trambaiolli, Tiago H. Falk, Francisco J. Fraga, Renato Anghinah, and Ana C. Lorena

Abstract— **There is recent indication that Alzheimer's disease (AD) can be characterized by atypical modulation of electrophysiological brain activity caused by fibrillar amyloid deposition in specific regions of the brain, such as those related to cognition and memory. In this paper, we propose to objectively characterize EEG sub-band modulation in an attempt to develop an automated noninvasive AD diagnostics tool. First, multi-channel full-band EEG signals are decomposed into five well-known frequency sub-bands: delta, theta, alpha, beta, and gamma. The temporal amplitude envelope of each sub-band is then computed via a Hilbert transformation. The proposed 'spectro-temporal modulation energy' feature measures the rate with which each sub-band is modulated. Modulation energy features are computed for 19 referential EEG signals and seven bipolar signals. Salient features are then selected and used to train four different classifiers, namely, support vector machines, logistic regression, classification and regression trees, and neural networks. Experiments with a database of 34 participants, 22 of which have been clinically diagnosed with probable-AD, show a neural network classifier achieving over 91% accuracy, thus significantly outperforming a classifier trained with conventional spectral-based features.**

I. INTRODUCTION

Recent statistics have placed Alzheimer's disease (AD) as the sixth leading cause of death in the United States and the third most expensive disease, after cardiovascular disease and cancer [1], [2]. It is estimated that 60-80% of dementia cases in North America are due to AD [1]. Commonly, AD results in memory loss and at least one more cognitive impairment, often leaving individuals unable to perform their daily activities. Early diagnosis is critical in order to initiate treatment that can significantly retard disease progression. Today, AD diagnosis may be done via neuropsychological evaluations, with accuracies ranging from 85-93% [3]. Definite diagnosis, however, can only be established with a histopathological analysis of the brain in which neurofibrillary tangles and neuritic plaques are found.

Since neuropsychological AD diagnosis demands long experimental sessions and experienced professionals, new non-invasive *automated* approaches have been sought. Recently, neuroimaging techniques, such as computerized tomography, magnetic resonance and positron emission tomography have emerged as promising candidates. The high cost of obtaining such equipment, however, has precluded its ubiquitous presence in clinics, particularly in developing countries. Moreover, recent research has suggested the limitations of neuroimaging techniques in accurately detecting tangles and plaques [4]. The use of quantitative electroencephalogram (EEG), on the other hand, has shown to be a viable less-costly alternative, with diagnostic accuracy inline with those obtained with more expensive neuroimaging techniques [5].

Conventionally, EEG analysis for automated AD diagnostics has fallen under two categories: spectral and nonlinear dynamics analysis [6]. With spectral analysis, the consensus is that EEG spectral power is reduced with AD in the alpha (8-12 Hz) and beta (12-30 Hz) frequency bands, and increased in the delta (0.1-4 Hz) and theta (4-8 Hz) bands. Spectral coherence (a measure of brain connectivity), in turn, has shown reduced values in AD when studying interhemispheric interactions, and has also been shown to be related to disease progression [6]. Nonlinear dynamics analysis, on the other hand, measures the complexity or chaoticity of the EEG signal. It has been shown that with AD, EEG complexity is decreased, possibly due to the reduced cortical interconnections resultant from the disease [6].

In this paper, we describe an alternate feature for EEG-based diagnosis of Alzheimer's disease, namely, spectro-temporal modulation energy. The development of the feature, which measures the rate of change of subband EEG modulations, was motivated by recent findings reported in the literature for AD treatment. In [7], deep brain stimulation was shown to *remodulate* brain activity in pathological areas affected by amyloid deposition and provided several clinical benefits, such as improvement or slowing of cognitive decline. The proposed feature, which conveys quantitative information of subband EEG modulation, is shown to be a useful metric for automated AD diagnosis.

II. MATERIALS AND METHODS

A. Participants

Thirty four participants volunteered for the study and provided written consent; ethics approval was obtained. Of these 34 participants, 22 were diagnosed with AD (age: 71.5 $\pm$ 7.7, 17 female) and 12 were age-matched healthy control (68.8 $\pm$ 6.7, 8 female). Alzheimer's disease diagnosis was made according to NINCDS-ADRDA [8] criteria and classified as mild to moderate, according to DSM III-R [9]. Participants had no history of other diseases and/or deficiencies that could also lead to cognitive impairment.

Lucas R. Trambaiolli and Ana C. Lorena are with the Mathematics, Computation and Cognition Center, Universidade Federal do ABC, Brazil. lucasrtb@yahoo.com, aclorena@gmail.com

Tiago H. Falk is with the Institut National de la Recherche Scientifique (EMT), University of Quebec, Canada. falk@emt.inrs.ca

Francisco J. Fraga is with the Engineering, Modeling and Applied Social Sciences Center, Universidade Federal do ABC, Brazil. franciscojfraga@gmail.com

Renato Anghinah is with the Reference Center of Behavioral Disturbances and Dementia, School of Medicine, Universidade de Sao Paulo, Brazil. anghinah@usp.br

978-1-4244-4122-8/11/$26.00 ©2011 IEEE

B. EEG capture and pre-processing

Nineteen channel EEG recordings were obtained with a *Braintech 3.0* instrumentation (EMSA Equipamentos Médicos Inc., Brazil), digitized with a 12-bit analog-to-digital converter and sampled at a rate of 200 Hz. Data was recorded with the participants awake and resting with their eyes closed. Placement of scalp electrodes followed the international 10-20 system and biauricular referential electrodes were used, resulting in 19 channels (referential montage), namely, Fp1, Fp2, F3, F4, F7, F8, C3, C4, T3, T4, T5, T6, P3, P4, O1, O2, Cz, Fz, Pz. An infinite impulse response low-pass elliptic filter with a zero at 60 Hz was applied to eliminate any power grid interference. For each participant, 40 eight-second artefact-free epochs were selected, per EEG channel, by an experienced physician.

An interhemispheric bipolar montage was also explored as there is growing evidence of an interhemispheric disconnection in AD. An EEG bipolar signal was obtained by subtracting the two bi-auricular referenced signals involved [10]. The following bipolar channels were used in this study: F3-F4, F7-F8, C3-C4, T3-T4, P3-P4, T5-T6, and O1-O2.

C. Spectro-temporal EEG amplitude modulation energy

As mentioned previously, there is growing evidence that brain activity modulation is compromised with AD [7]. Here, we propose a novel feature for AD diagnosis which quantitatively monitors EEG amplitude modulation. The feature is termed 'EEG spectro-temporal modulation energy'; Figure 1 depicts the signal processing steps involved in its computation. First, the full-band EEG signal is decomposed into five well-known sub-bands: delta (0.1-4 Hz), theta (4-8 Hz), alpha (8-12 Hz), beta (12-30 Hz), and gamma (30-100 Hz). The temporal amplitude envelope of each sub-band signal is then computed by means of a Hilbert transform [11]. In order to quantify the rate of change of the sub-band temporal envelopes, we further decompose the envelopes into five so-called modulation bands and compute the energy present in each modulation band.

The resultant spectro-temporal modulation representation conveys rate-of-change information for each of the five sub-band amplitude envelopes. In this study, the frequency range of modulation bands are empirically set to coincide with the frequency range of conventional bands. To distinguish between the two, however, modulation bands are appended by a prefix "m-" (e.g., m-delta, 0.1-4 Hz). In order to perform automated AD diagnosis, 25 modulation energy features are computed for each of the 19 EEG channels, as well as the seven bipolar signals. The features represent the percentage of the overall modulation energy present in each of the five frequency and five modulation-frequency bands.

D. Salient feature selection and classifier design

A total of 650 modulation energy features (25 features $\times$ [19 channels + 7 bipolar signals]) were extracted per epoch, per participant. In order to reduce such high-dimensional feature space into one that is feasible for classifier design, correlation-based feature selection using a genetic search

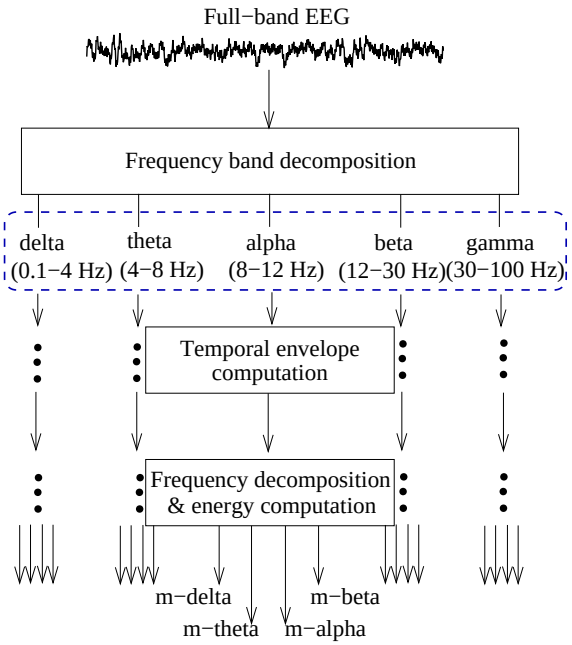

Fig. 1. Signal processing steps comprised in the calculation of EEG spectro-temporal modulation energy.

paradigm was used to select salient features and to prune redundant ones. Of the 40 EEG epochs available for each participant, 10 were set aside for feature selection; the remaining 30 were used for classifier training and testing (in leave-one-out-patient tests). Once salient features were selected, four classification algorithms were tested for automated AD diagnosis. The Weka implementation [12] of support vector classifier (SVC), logistic regression (LR), classification and regression tree (CART), and neural network (NN) classifiers were tested. To allow for a fair comparison between different classifiers, default settings were used; further improvements are warranted once parameter optimization is in place.

III. EXPERIMENTAL RESULTS

A. Feature selection

Table I shows the top 33 features (and their ranks) selected in our experiment; this number of features is inline with those previously reported in the literature (e.g., [13]). In the table, features are represented as "Pos-Band-ModBand," where 'Pos' indicates the electrode position (e.g., O1) or the bipolar signal (e.g., T5-T6), 'Band' indicates the frequency band, and 'ModBand' the modulation band. As can be seen, occipital region information achieved the two highest feature ranks, with features encompassing both the referential and bipolar montage assemblies (O1 and O1-O2, respectively).

B. Diagnostic performance

As mentioned previously, the available dataset consisted of 1360 8-second EEG epochs (40 epochs per participant, 34 participants). Of these, 340 (10 epochs per participant) were used for feature selection and the remaining 1020 were left for classifier design and testing. Here, a leave-one-patient-out (LOPO) approach was used for classifier training/testing.

TABLE I

TOP 33 MODULATION ENERGY-BASED FEATURES SELECTED VIA CORRELATION-BASED FEATURE SELECTION USING A GENETIC SEARCH PARADIGM.

Feature	Rank	Feature	Rank	Feature	Rank
O1−theta−m-beta	1	Fz−beta−m-theta	12	Fz−gamma−m-theta	23
O1-O2−theta−m-theta	2	O1-O2−gamma−m-alpha	13	P3-P4−theta−m-delta	24
C3-C4−beta−m-delta	3	T3-T4−alpha−m-delta	14	P4−theta−m-delta	25
P3-P4−beta−m-delta	4	C4−delta−m-alpha	15	T5-T6−beta−m-delta	26
F3-F4−theta−m-alpha	5	C4−delta−m-beta	16	T6−delta−m-beta	27
Fz−theta−m-alpha	6	P3−delta−m-theta	17	T6−beta−m-theta	28
T3-T4−alpha−m-alpha	7	Pz−beta−m-theta	18	C4−theta−m-alpha	29
F7−theta−m-delta	8	T3-T4−beta−m-alpha	19	C4−theta−m-beta	30
Fz−beta−m-delta	9	F3−theta−m-delta	20	F7−alpha−m-delta	31
T4−gamma−m-theta	10	F8−theta−m-delta	21	F8−beta−m-theta	32
F7−alpha−m-theta	11	F8−gamma−m-beta	22	Fz−delta−m-theta	33

LOPO is useful as it assesses the generalization ability of the classifier as well as its diagnostic performance for "unseen" patients. In each of the 34 runs of the train/test process, 990 of the epochs are kept for training and the remaining 30 are left for testing. At each run, the test set consists of data from a participant that is unseen to the classifier.

Three performance metrics were used, namely, overall accuracy, sensitivity (percentage of correctly classified epochs belonging to AD patients), and specificity (percentage of correctly classified epochs belonging to healthy patients), all expressed in percentage values. Tables II and III show the performance obtained with the pre-selected modulation energy features using referential, bipolar, or combined referential-bipolar montage assemblies. Table II presents results on a per-epoch basis while Table III presents classifier performance on a more medically relevant "per-participant" basis. In the per-participant case, a patient is deemed to be correctly classified when 50% or more of its 30 epochs have been correctly classified.

IV. DISCUSSION

A. Salient features

As can be seen from Table I, the electrode positions selected most often (Fz, F7, F8) were associated with the frontal region. These findings corroborate those reported in [14], [15] where significant differences in brain activity and EEG spectral power were reported in the midfrontal and frontal lobes between AD and healthy control patient groups. These findings suggest that with AD, not only is EEG spectral power affected, but so is EEG power modulation. The most significant feature, on the other hand, corresponded to modulation information extracted from the left occipital region, thus inline with results reported recently using EEG complexity parameters [16]. Moreover, all bipolar signals, with the exception of F7-F8 were selected.

Modulation information extracted from the theta and beta frequency bands were selected most often, whereas the opposite was observed with the alpha and gamma bands. Interestingly, theta-beta coupling has been shown in the past to be related to working memory performance [17] and to affect and emotion regulation [18], two prominent characteristics in AD. As for modulation bands, information extracted from m-delta and m-theta bands were selected most often and m-gamma information was completely discarded. These findings suggest that slowly-varying EEG amplitude modulations are the ones mostly affected by AD; these findings may be useful to guide AD treatment interventions, such as those described in [7].

B. Classifier performance

As observed from Tables II and III, the four classifiers obtained similar performances, with neural networks achieving somewhat better results across the three performance metrics and support vector classifiers achieving better sensitivity levels. In the per-participant case, neural networks with a combined referential-bipolar montage assembly achieved over 90% performance on all three performance metrics. The results reported here with the proposed modulation energy-based features compare favorably against results reported on the same dataset using conventional spectral-based measures. As an example, 81.2%, 82.5%, and 80.2% were reported in [19] for diagnostic accuracy, sensitivity, and specificity, respectively, using spectral peak and coherence as features and support vector machines as classifiers. Lastly, it was also observed that high accuracy and sensitivity levels could be obtained with the bipolar signals alone. Since the bipolar montage measures EEG regional potentials [10], an inter-hemispheric disconnect may indeed be present with AD.

C. Limitations and ongoing investigations

Findings reported here were based on a limited gender-unbalanced sample size of 34 participants; a larger participant pool is needed in order to explore if modulation energy features are reliable for AD diagnosis as well as to monitor disease progression. Moreover, the artefact-free EEG epochs used here were selected by an experienced physician. In order to make the diagnostic system completely automated, artefact removal should be achieved by means independent component analysis (ICA) [20]; this is the focus of our

TABLE II

PERFORMANCE OF PROPOSED FEATURES USING THE REFERENTIAL, BIPOLAR, AND COMBINED REFERENTIAL-BIPOLAR FEATURE SUBSETS. PERFORMANCE IS REPORTED ON A PER-EPOCH BASIS AND REPRESENTS THE (MEAN $\pm$ STANDARD DEVIATION) OVER ALL PARTICIPANTS.

Classifier	Referential (%)			Bipolar (%)			Combined (%)		
	Accuracy	Sensitivity	Specificity	Accuracy	Sensitivity	Specificity	Accuracy	Sensitivity	Specificity
SVC	78.9 ± 36.2	87.3 ± 28.4	63.6 ± 44.7	81.3 ± 27.3	89.1 ± 18.6	67.2 ± 35.2	85.9 ± 30.6	93.6 ± 21.7	71.9 ± 39.6
LR	78.3 ± 25.7	82.7 ± 23.3	70.2 ± 28.8	82.6 ± 29.5	87.2 ± 26.4	74.1 ± 33.9	79.4 ± 27.5	78.6 ± 28.6	80.8 ± 26.6
CART	71.2 ± 34.2	78.4 ± 30.2	58.1 ± 38.3	78.0 ± 27.3	83.4 ± 23.8	68.1 ± 31.5	71.2 ± 36.9	77.7 ± 32.6	59.4 ± 42.8
NN	82.9 ± 28.2	86.9 ± 23.7	75.5 ± 34.9	82.3 ± 26.5	87.7 ± 16.2	72.5 ± 38.1	87.1 ± 24.9	88.3 ± 25.1	85.0 ± 25.4

TABLE III

PERFORMANCE OF PROPOSED FEATURES USING THE REFERENTIAL, BIPOLAR, AND COMBINED REFERENTIAL-BIPOLAR FEATURE SUBSETS. PERFORMANCE IS REPORTED ON A PER-PARTICIPANT BASIS.

Classifier	Referential (%)			Bipolar (%)			Combined (%)		
	Accuracy	Sensitivity	Specificity	Accuracy	Sensitivity	Specificity	Accuracy	Sensitivity	Specificity
SVC	79.41	86.36	66.67	82.35	95.45	58.33	88.24	95.45	75.00
LR	85.29	90.91	75.00	85.29	90.91	75.00	82.35	81.82	83.33
CART	70.59	77.27	58.33	79.41	81.82	75.00	67.65	72.73	58.33
NN	82.35	86.36	75.00	91.18	95.45	83.33	91.18	90.91	91.67

ongoing work. Future works also shall consider comparisons with linear and nonlinear measures.

V. CONCLUSIONS

In this paper, a new feature for automated EEG-based Alzheimer disease (AD) diagnosis is proposed. The feature, termed "spectro-temporal modulation energy," measures the rate with which EEG sub-band signals are modulated. Experiments with a multi-channel EEG database measured from 34 participants (12 control, 22 probable-AD) show that a neural network classifier, trained on salient features extracted from different brain regions, can achieve significantly higher diagnostic accuracy relative to classifiers trained on conventional spectral-based features (i.e., spectral peaks and coherence). The automated tool has the potential to assist physicians in AD diagnosis, evaluation of treatment outcomes, as well as in providing a means to dispense with time-consuming and resource-intensive neuropsychological assessments.

REFERENCES

[1] Alzheimer Association, "Alzheimer's disease facts and figures: 2010 report," *Alzheimers Dement*, vol. 6, no. 2, pp. 158–194, 2010.

[2] B. Leifer, "Early diagnosis of Alzheimer's disease: clinical and economic benefits," *J Am Geriatr Soc*, vol. 51, pp. 281–288, 2003.

[3] D. Parikh *et al.*, "Ensemble-based data fusion for early diagnosis of Alzheimers disease," *Proc Intl Conf IEEE-EMBS*, pp. 2479–2482, 2005.

[4] Z. Sankari, H. Adeli, and A. Adeli, "Intrahemispheric, interhemispheric, and distal EEG coherence in Alzheimers disease," *Clin Neurophysiol*, 2010, , in press, doi:10.1016/j.clinph.2010.09.008.

[5] H. Adeli, S. Ghosh-Dastidar, and N. Dadmehr, "Alzheimer's disease: models of computation and analysis of EEGs," *Clin EEG Neurosci*, vol. 36, no. 3, pp. 131–140, 2005.

[6] J. Jeong, "EEG dynamics in patients with Alzheimer's disease," *Clin Neurophysiol*, vol. 115, no. 7, pp. 1490–1505, 2004.

[7] A. Laxton *et al.*, "A phase I trial of deep brain stimulation of memory circuits in Alzheimer's disease," *Ann Neurol*, vol. 68, no. 4, pp. 521–534, 2010.

[8] G. McKhann, D. Drachman, M. Folstein, R. Katzman, D. Price, and E. Stadlan, "Clinical diagnosis of Alzheimer's disease: Report of the NINCDS-ADRDA Work Group," *Neurology*, vol. 34, no. 7, pp. 939–944, 1984.

[9] R. Spitzer and J. Williams, *User's guide for the structured clinical interview for DSM-III-R*. American Psychiatric Publishing, Inc., 1990.

[10] L. Trambaiolli, A. Lorena, F. Fraga, P. Kanda, R. Nitrini, and R. Anghinah, "Does EEG montage Influence Alzheimers Disease electroclinic diagnosis?" *Int J Alzheimer's Disease*, 2011, in press.

[11] M. Le Van Quyen, J. Foucher, J. Lachaux, E. Rodriguez, A. Lutz, J. Martinerie, and F. Varela, "Comparison of Hilbert transform and wavelet methods for the analysis of neuronal synchrony," *J Neurosci Meth*, vol. 111, no. 2, pp. 83–98, 2001.

[12] E. Frank, M. Hall, G. Holmes, R. Kirkby, B. Pfahringer, I. Witten, and L. Trigg, *Data Mining and Knowledge Discovery Handbook*. Springer, 2010, ch. Weka-a machine learning workbench for data mining, pp. 1269–1277.

[13] C. Lehmann *et al.*, "Application and comparison of classification of alzheimers disease in electrical brain activity (eeg)," *J Neurosci Meth*, vol. 161, pp. 342–350, 2007.

[14] F. Duffy, M. Albert, G. McAnulty, and A. Garvey, "Age-related differences in brain electrical activity of healthy subjects," *Annals of neurology*, vol. 16, no. 4, pp. 430–438, 1984.

[15] C. Babiloni, G. Binetti, A. Cassarino, G. Dal Forno, C. Del Percio, F. Ferreri, *et al.*, "Sources of cortical rhythms in adults during physiological aging: a multicentric EEG study," *Hum Brain Map*, vol. 27, no. 2, pp. 162–172, 2006.

[16] H. Adeli, S. Ghosh-Dastidar, and N. Dadmehr, "A spatio-temporal wavelet-chaos methodology for EEG-based diagnosis of Alzheimer's disease," *Neurosci lett*, vol. 444, no. 2, pp. 190–194, 2008.

[17] N. Axmacher, M. Henseler, O. Jensen, I. Weinreich, C. Elger, and J. Fell, "Cross-frequency coupling supports multi-item working memory in the human hippocampus," *P Natl Acad Sci USA*, vol. 107, no. 7, p. 3228, 2010.

[18] P. Putman, J. van Peer, I. Maimari, and S. van der Werff, "EEG theta/beta ratio in relation to fear-modulated response-inhibition, attentional control, and affective traits," *Biol Psychol*, vol. 83, no. 2, pp. 73–78, 2010.

[19] L. Trambaiolli, A. Lorena, F. Fraga, and R. Anghinah, "Support Vector Machines in the Diagnosis of Alzheimer's Disease," in *Proc ISSNIP Biosignals and Biorobotics Conf.*, vol. 1, 2010, pp. 1–6.

[20] C. Melissant, A. Ypma, E. Frietman, and C. Stam, "A method for detection of Alzheimers disease using ICA-enhanced EEG measurements," *Artif Intel Med*, vol. 33, no. 3, pp. 209–222, 2005.